Dust emission variability at the Salton Sea, California, USA

DATASET · MAY 2014

5 AUTHORS, INCLUDING:

James King
Université de Montréal
40 PUBLICATIONS **258** CITATIONS
SEE PROFILE

Mark Sweeney
University of South Dakota
25 PUBLICATIONS **262** CITATIONS
SEE PROFILE

Brenda Buck
University of Nevada, Las Vegas
84 PUBLICATIONS **581** CITATIONS
SEE PROFILE

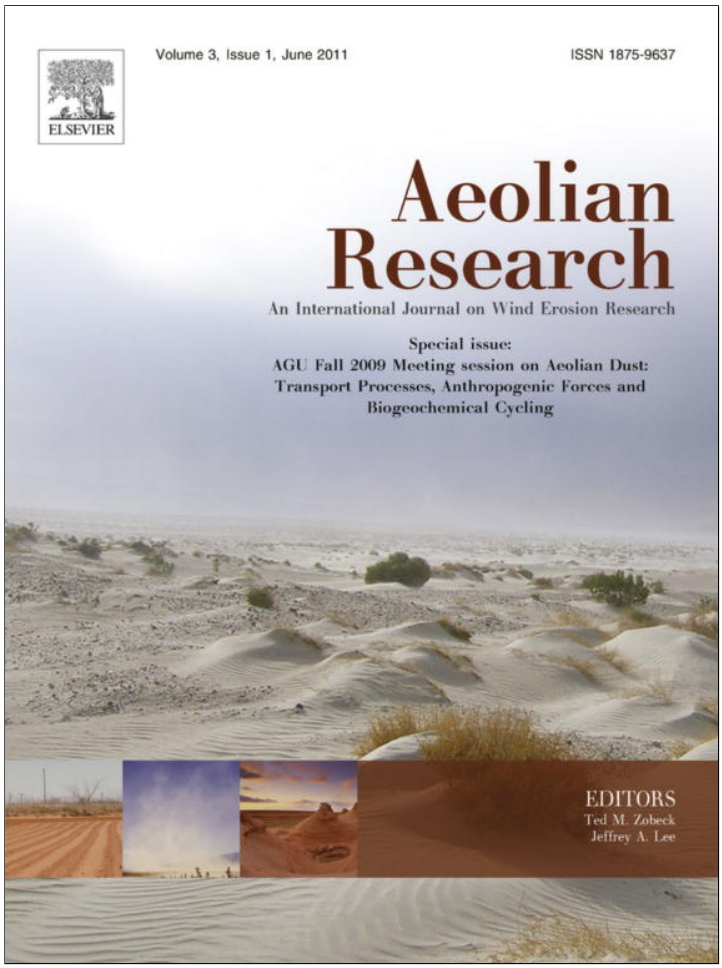

Aeolian Research 3 (2011) 67–79

Contents lists available at ScienceDirect

Aeolian Research

journal homepage: www.elsevier.com/locate/aeolia

Dust emission variability at the Salton Sea, California, USA

James King [a,*], Vic Etyemezian [a], Mark Sweeney [b], Brenda J. Buck [c], George Nikolich [a]

[a] Division of Atmospheric Sciences, Desert Research Institute, 755 E. Flamingo Rd., Las Vegas, NV 89119, USA
[b] Department of Earth Sciences, University of South Dakota, 414 E. Clark St., Vermillion, SD 57069, USA
[c] Department of Geosciences, University of Nevada Las Vegas, 4505 Maryland Parkway, Las Vegas, NV 89154, USA

ARTICLE INFO

Article history:
Received 14 September 2010
Revised 19 January 2011
Accepted 7 March 2011
Available online 19 April 2011

Keywords:
PM10
Aeolian
Windblown dust
Fugitive dust
Emission inventory
Wind tunnel

ABSTRACT

A field study conducted through a series of four field campaigns between 2005 and 2007 investigated the potential for dust emissions around the Salton Sea in California, USA. This paper explores the landform related controls on fugitive PM_{10} dust emissions from soil surfaces surrounding the Salton Sea by measuring soil properties combined with estimating the in situ PM_{10} dust emissions using a novel small portable field wind tunnel (PI-SWERL). The locations surrounding the Salton Sea were selected to encompass varying geomorphic landforms, including exposed shoreline areas with playa characteristics, barnacle covered beaches, dry washes, interdunes, and exposures of ancient Lake Cahuilla. The largest variation in potential dust emissions over the sampling period was from the playa-like surfaces that are near the open water and exhibited surface salt crusts, with the highest emissions measured from these surfaces during the winter. However, the largest emitting landform over the entire period were the dry washes that only exhibited a small degree of silt/clay crust, if any and were composed mainly of sand-sized particles. The highest emissions from all surfaces are compared with dust fluxes measured from Owens Lake and are within the same order of magnitude as those also measured with wind tunnels. Salt content did not show any statistically significant correlation with PM_{10} dust emissions during any sampling period for the soils tested, which is attributed to the complications associating soil salt contents with particular salt crystal habit.

1. Introduction

The Salton Sea (Fig. 1) is a terminal lake that was inadvertently formed during the diversion of the Colorado River in the early part of the 20th century. Since then, its waters have been increasing in salinity (Schoeder et al., 2002). A reduction in agricultural runoff by improved water conservation practices, combined with a constant inflow of salts, will potentially decrease lake levels, while salinity will continue to increase. Also, in partial fulfillment of the Colorado River Quantification Settlement Agreement (QSA), water inflow into the Salton Sea is slated to be significantly reduced starting in 2018. In addition to these longer-term reductions in inflows, the Salton Sea shoreline environment is also subject to change on shorter time scales owing to seasonal trends in precipitation and water inflows. As waters recede, salt crystals precipitate on the recently exposed shorelines. The chemical, mineral, and morphological compositions of these salts are likely to have a profound influence on whether or not recently exposed shorelines will become a more or less significant source of windblown dust. An important air quality concern is the potential for increased windblown dust emissions from locations where currently submerged areas would be uncovered, periodically or permanently, as the Salton Sea shoreline transforms under these changing inflow conditions.

A series of field studies were conducted between September 2005 and February 2007 around the Salton Sea to help assess the potential seasonal variability of dust emissions as the water level and water quality change. The potential for PM_{10} (i.e., particulate matter with aerodynamic diameter equal to, or smaller than, 10 μm) dust emissions was directly measured at the same sites to provide an estimate of the magnitudes and variability of windblown dust potential from recently exposed shorelines.

This investigation was divided into four field campaigns representing the fall, winter, and early spring season, with an additional visit in the spring season of the following year, to capture the dependence of dust emissions on environmental factors. The objectives were to: (i) measure the dust emissions from a selection of locations on the Salton Sea shoreline by season; and (ii) investigate any correlations between dust emissions and landforms (based on simple measured soil properties) at the Salton Sea, with emphasis on the areas that are recently exposed. Results of extensive salt crust analyses are provided in a separate manuscript (Buck et al., in press).

* Corresponding author.
E-mail address: james.king@dri.edu (J. King).

1875-9637/$ - see front matter © 2011 Elsevier B.V. All rights reserved.
doi:10.1016/j.aeolia.2011.03.005

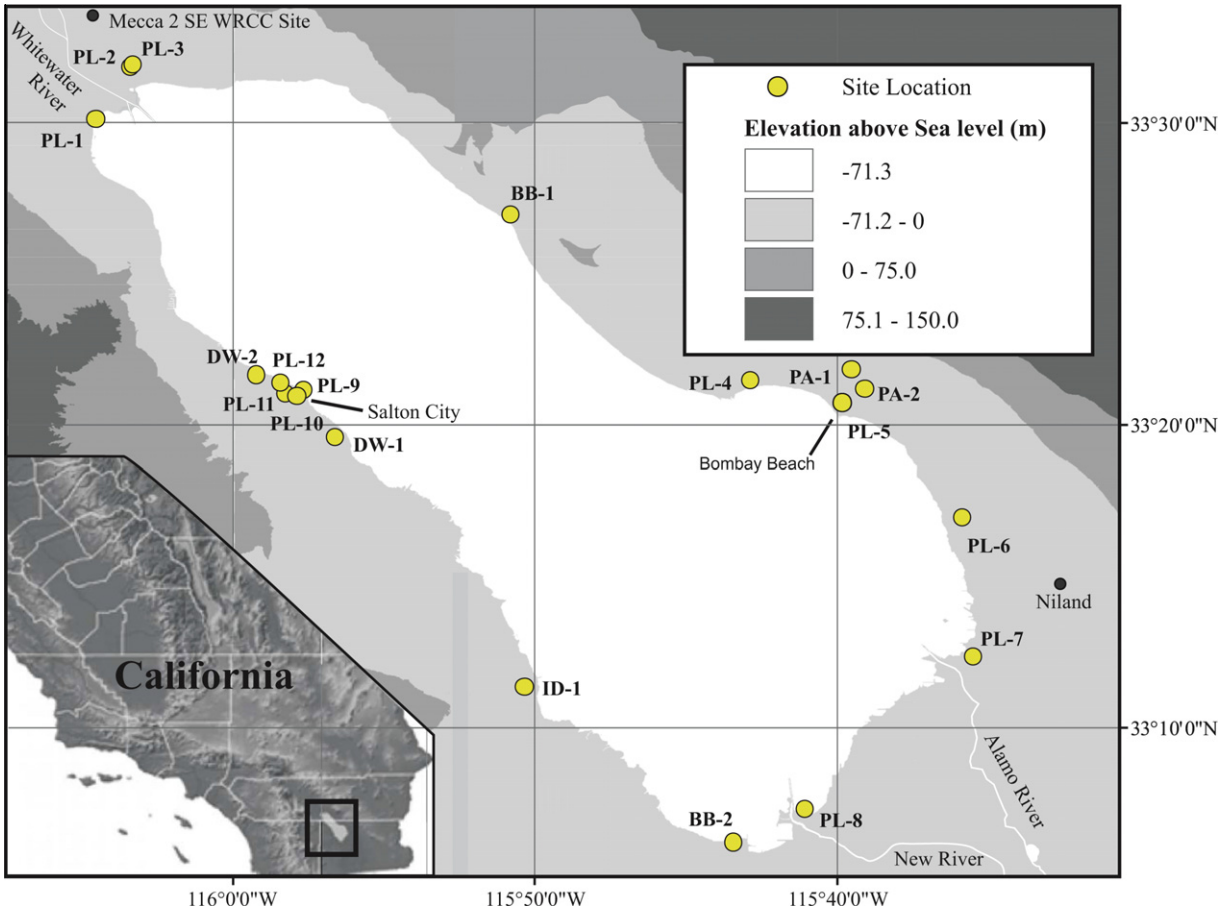

Fig. 1. Map of Salton Sea with site locations.

2. Background

2.1. Location

The Salton Sea is located in the northern portion of the Imperial Valley and is approximately 970 km^2 in area with a maximum depth of 15 m. Prior to its flooding in 1905 by the overflow of the Colorado River, the Salton Sink basin was the site of a major salt mining operation. Older sediments exposed along the shoreline record multiple Holocene and Pleistocene lacustrine episodes (Babcock, 1974). The Quantification Settlement Agreement, which details the allocation of portions of the Colorado River between the local water districts and authorities, mandates that the surface water level should be maintained at −69.2 m above sea level or higher until 2018. However, seasonal variations in the agricultural runoff result in distinct high and low water level periods at the Salton Sea that increase the exposed land surfaces near the shoreline during the low water period (late summer through winter). Some of these relatively flat, seasonally exposed areas can be described as playa-like because of their fine sediment composition, proximity to groundwater, high salt content, and ultimately their susceptibility to wind erosion. Playas that are close to the groundwater level have been found to be seasonally susceptible to wind erosion within the southwest U.S. (Gill, 1996; Pelletier, 2006; Reynolds et al., 2007), and quick exposure of larger areas (such as in the case of Owens Lake) can, without proper mitigation, lead to severe dust emissions. Although only a portion of the formerly submerged Salton Sea area is presently exposed, the rate at which it is being exposed has increased in the last 5 years, prompting interest in the potential air quality issues from the newly exposed surfaces.

2.2. Sediment transport

Fugitive dust emissions from semi-arid and arid surfaces occur from two main processes: (1) The direct entrainment of dust by aerodynamic forces, resulting in a relatively small vertical dust flux (nominally, dust mass emitted per unit area per unit time) for a given wind speed (Loosemore and Hunt, 2000); and (2) sandblasting or saltation bombardment that creates much higher dust fluxes by the impact of larger sand-sized aggregates which abrade finer surface sediments and themselves break up into finer particles (Gillette and Walker, 1977; Shao et al., 1993). Larger soil particles, such as sand, have a lower fluid threshold and once in motion are capable of efficiently transferring the wind's momentum to the soil surface (Bagnold, 1941) by impacting the soil surface and causing emissions of other particles with a size distribution that is dependent on the soil type (Lu and Shao, 1999). For silt- or clay-rich soils, substantially higher shear velocities (u^* – a measure of momentum transfer from the wind to the surface) are typically required to initiate particle motion owing to the high cohesive forces usually associated with silt and clay particles. If present, a salt crust composed of interlocking crystals can additionally increase the shear velocity required for transport. Nevertheless, some portion of dust particles on a soil surface is amenable to direct entrainment, and the magnitude of wind required for such entrainment can be substantially lower than that required to initiate saltation (Nickling et al., 1997; Etyemezian et al., 2006).

For either process, a 'binding energy' must be overcome to liberate a significant mass from a surface that contains the dust-sized particles (Gillette, 1979; Gomes et al., 1990; Shao et al., 1993). The magnitude of this binding energy is highly variable and is dependent on sediment size populations, moisture availability, organic

matter content, surface crusts from salt or microbial content (a function of salt mineralogy, groundwater or perched water levels, and soil processes), and the quantity and availability of loose sand-sized sediment (Nickling, 1984; Gillette and Chen, 1999; Rice and McEwan, 2001; Okin, 2005). Accounting for all of these factors in a predictive model has proven very difficult and is generally unrealistic (Shao and Lu, 2000). Therefore, various parameters have been developed as surrogates for the resistance of a surface to entrainment and are used in sediment entrainment and dust flux equations. These include the modulus of rupture, which is indirectly measured with a soil penetrometer (Gillette et al., 1982; Houser and Nickling, 2001; Langston and McKenna Neuman, 2005), and the binding energy, which is calculated through the theoretical development of a model based on impact energy from saltating grains and energy released from dust particles (Rice et al., 1999; Shao et al., 1993). However, these surrogate measurements are indirect; they only provide information on the bulk surface strength, whereas the process of sandblasting emits dust by gradually eroding weaker parts of the surface and preferentially exposing different portions of the soil profile.

Salt minerals in soils can exert a profound influence on both the amount of fine material available for aeolian erosion and on the spatial and temporal distribution of dust emissions (Gillette et al., 2004; Langston and McKenna Neuman, 2005; Reynolds et al., 2007). Salt minerals are common components in arid soils, and their high solubility can result in significant variation in soil characteristics over very short time periods and distances (Buck et al., 2006). Preliminary data suggest that under certain climatic conditions, salt minerals may precipitate as loose, unconsolidated, individual, silt- to sand-sized crystals, or they can form a hard crust composed of interlocking crystals. In the context of dust emissions, a potentially more important factor than mineralogy is the interlocking nature of precipitated crystals (Buck et al., in press). If crystals are small but in an interlocking form, then they can still form a very hard crust. Thus, the presence or absence of salt crusts as well as the size and interlocking nature of the precipitated crystals will control to a large extent the amount of dust particles that are available for suspension (Buck et al., in press), and these salt crust variables can vary on many different time scales.

3. Methods

The purpose of the Salton Sea field measurements was to provide insights into the relationships between season, soil properties, and windblown dust emissions. Therefore, wherever possible, all field sampling sites were characterized for soil textural properties, soil bulk density, surface crust properties, soil salt content, and PM_{10} dust emissions. However, because of the complexities associated with dust emissions and soil properties in field environments the aim of the methodology was to account for properties that would account for most of the variation in emissions and that were easily measureable. Four separate field sampling campaigns broadly representing the different seasonal conditions of fall, winter (repeated), and spring when conditions for dust emissions are most optimal were completed in 2005 through 2007. The field measurement periods were: September 21–30, 2005 (SE05), January 24–27, 2006 (JA06), March 20–24, 2006 (MR06), and February 8–11, 2007 (FE07). The sampling period of FE07 utilized a slightly different methodology mainly because of the changing nature of the landscape and additional objectives when conducting soil analyses.

3.1. General site methodology

The general methodology followed at each location included these steps: (1) the uppermost surface crust was collected for physical soil properties and chemical analysis; (2) a shallow (less than 30 cm) soil pit was dug to characterize the bulk soil properties including grain size, and the upper soil profile; (3) potential dust emissions were measured by the PI-SWERL wind tunnel; and (4) the location (via GPS), relative elevation, and distance from the shoreline (when applicable) were measured.

3.2. Locations

Sites were selected to meet the following criteria: (1) accessibility, (2) permission of landowners, (3) inclusion of a wide variety of soil textures, and (4) inclusion of several recently exposed shorelines with playa-like characteristics. Shorelines that are periodically inundated with water due to seasonal rises and falls of the Salton Sea display features similar to playas (hereafter referred to as playa-like or PL) including fine-grained sediment textures, mudcracks, and physical surface crusts. Some shoreline sites were armored with barnacles, reflecting higher wave energy (referred to as a barnacle beach, BB). In an attempt to capture some variability in the emissions around the Salton Sea, we also chose sites in dry, ephemeral washes (dry wash, DW), interdune areas (interdune, ID), and exposed sediments from ancient Lake Cahuilla (paleolake, PA), which were predominantly exposed on the eastern shoreline. Based on the above criteria 14 sites were initially selected for measurement of windblown dust emission potential (Fig. 1). The restrictions from the above site criteria and in the aim of sampling a variety of surfaces within the basin resulted in a selection that cannot be considered spatially unbiased. During the subsequent JA06 field campaign, three additional sites (PL-9, PL-10, and PL-12) were added to the preliminary list to emphasize salt-crusted playa-like surfaces that may have been under-represented in the initial site selection. In addition, during the FE07 campaign, two sites were added (PL-2 and PL-3), and ten of the original sites were re-visited; during this campaign. At many sites, field visits were not accessible other than at times of year with lower water levels (generally winter) and therefore were not sampled. The sites not sampled during the FE07 campaign (all but PL sites) were deemed from the previous three measurement campaigns to be adequately described and therefore new PL sites were measured instead. Measurement locations are shown in Fig. 1.

3.3. On-site measurements

Two soil pits 30 cm deep were dug at each site to describe bulk soil properties (moisture, hardness, textural changes), and surface soil properties, such as crust thickness, crust type, and subcrust. Samples were collected for textural and chemical analysis (methods explained in Section 3.4).

The PM_{10} emissions were measured using the Portable In-Situ Wind Erosion Lab (PI-SWERL, Etyemezian et al., 2006, 2007; Sweeney et al., 2008). The PI-SWERL is a variable direct current battery powered instrument that creates a shear stress on the ground surface within a cylindrical enclosure using a rotating annular blade within close proximity of the surface. It measures the PM_{10} concentration (C, g/m^3) at an outlet with a DustTrak that records at 1 Hz while a blower vents filtered air (measurements are made on calm days only to minimize venting high PM_{10} concentrated air) through the PI-SWERL at a constant rate (F, m^3/s). By calibrating the PI-SWERL PM_{10} emissions with the University of Guelph field wind-tunnel (Sweeney et al., 2008), and the RPM with shear stress measurements made under the PI-SWERL in the laboratory (Etyemezian et al., 2007), C and F can be converted into an emission flux (g/m^2/s) or amount of PM_{10} per area per second by:

$$E_{i,cum} = \frac{\sum_{begin,1}^{end,i} C \times F}{t_{end,i} - t_{begin,i}} \Big/ A_{eff} \quad (1)$$

where the summation occurs over every 1-s measurement during level i, beginning at $t_{begin,i}$ and ending at $t_{end,i}$, with t as integer seconds. The measured dust concentration and flow rate are converted to an emission flux by the effective area of the PI-SWERL, A_{eff}, which is 0.07 m^2. A test sequence and the calculated E_i for each step increase in PI-SWERL speed and equivalent shear velocity (u^*) are shown in Fig. 2 for a typical emission time series on an emissive surface. The PI-SWERL was operated at every site that was dry enough for testing during each of the field sampling campaigns. For ease of movement, the PI-SWERL unit was mounted onto the front end of an ATV.

The PI-SWERL was operated at pre-set RPM intervals, where each RPM level was held for between 180 and 300 s (lower RPM settings held for shorter periods of time). The maximum RPM during testing changed based on the upper PM_{10} concentration measurement limit for the DustTrak (0.150 g/m^3). During each measurement campaign, between 3 and 12 replicate measurements with the PI-SWERL were completed at each site. The emission estimates collected at each site for one field visit, were treated as replicate measurements and log-transformed for all multivariate statistical analyses to satisfy the assumption of normal distribution. Aggregated values of potential dust emissions from each site were achieved using the geometric mean (average of the logarithmic values, raised to the exponent of 10). The geometric mean approach is useful for viewing the data and calculating statistics from a study when those data vary by many orders of magnitude in value. All statistical analyses were processed using Matlab® (The Mathworks Inc.).

3.4. Laboratory analyses

The laboratory tests for all field campaigns included moisture content, texture, calcium carbonate percent, organic carbon percentage, and saturated paste pH and electrical conductivity (EC) using a 1:1 ratio with Reverse Osmosis water. Soil samples for all these tests were obtained from the bulk sampling at each site during each field campaign. Some differences in the values may have been caused by spatial heterogeneity since the exact location of bulk samples may have changed because of accessibility. In the lab, soil samples were weighed, dried for 24 h at 105 °C, and weighed again to determine gravimetric moisture content. Particle size distribution of the fine fraction (<2 mm) was determined using a combination of standard dry sieves and laser diffraction techniques (Gee and Or, 2002) for all but the last field campaign (texture was determined by hydrometer method for those samples). In the case of the first three field campaigns, the dry sieve method was used to determine the coarse to very fine sand fractions in the samples. Laser particle size analysis was used to determine the distribution of coarse sand and less (including silt and clay sized particles) within the samples using a Micromeritics Saturn DigiSizer 5200. The sample was internally dispersed using ultra-sonication in de-ionized water with 0.005% surfactant (sodium metaphosphate) and circulated through the path of the laser light beam. The Micromeritics Saturn DigiSizer 5200 calculates the diameter of a particle as if it were a sphere.

Percentage of calcium carbonate in the soils was determined by acid digestion in a Chittick apparatus to measure the volume of CO_2 gas evolved (Dreimanis, 1962; Machette, 1986) during the first three field seasons, and gravimetric loss after dissolution with a sodium acetate buffer solution for the last field season (Kunze and Dixon, 1986). Salt content was estimated from electrical conductivity (EC) of aqueous soil extracts for the first three field seasons, and gravimetric loss after dissolution with RO water for the last field season (Soukup et al., 2008). Salt contents are roughly equivalent to NRCS soil description guidelines: nonsaline (<1000 mg/kg, EC 0–2 mmhos/cm), very slightly saline (1000–10,000 mg/kg, EC 2–4 mmhos/cm), slightly saline (10,000–25,000 mg/kg, EC 4–8 mmhos/cm), moderately saline (25,000–50,000, EC 8–16 mmhos/cm), and strongly saline (>50,000 mg/kg, EC > 16 mmhos/cm) (Richards, 1954; Soil Survey Division Staff, 1993). Water containing dissolved salts conducts current proportional to the amount of salt present. A soil–water extract of 1:5 (1:1 for the FE07 campaign) was used in conjunction with a conductivity bridge to estimate the total amount of soluble salt. Hydrogen-ion

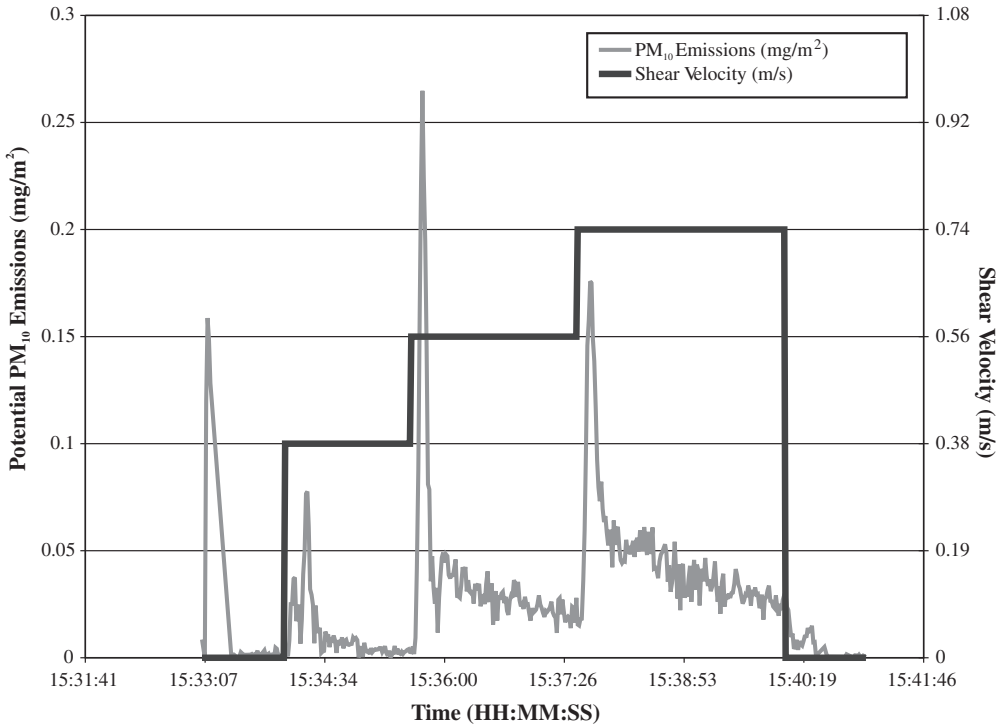

Fig. 2. PI-SWERL test sequence.

Table 1
Site locations (coordinates in decimal degrees), elevation above the Salton Sea water level (approximate) and characteristics.

Site	Latitude	Longitude	Elev. (m)	Site Visit Schedule				Land form	Crust Type
				SE05	JA06	MR06	FE07		
DW-1	33.32312	−115.94570	3.0	X	X	X		Dry wash	n/a
DW-2	33.35265	−115.97265	2.7	X	X	X		Dry wash	n/a
PA-1	33.36175	−115.66695	8.0	X	X	X		Paleolake	Silt/clay
PA-2	33.35018	−115.65553	8.0	X	X	X	X	Paleolake	Silt/clay
PL-1	33.4974	−116.07981	0.3	X	X	X	X	Playa-like	Salt
PL-2	33.53033	−116.05792	0.3				X	Playa-like	Salt
PL-3	33.52963	−116.05980	0.3				X	Playa-like	Salt
PL-4	33.35416	−115.72106	1.0	X	X	X	X	Playa-like	Salt
PL-5	33.341	−115.66796	1.0	X	X	X	X	Playa-like	Salt
PL-6	33.27812	−115.60220	0.3	X			X	Playa-like	Salt
PL-7	33.20039	−115.59705	0.3	X	X	X	X	Playa-like	Salt
PL-8	33.11743	−115.69131	0.3	X	X	X	X	Playa-like	Salt
PL-9	33.34838	−115.96549	0.3		X	X	X	Playa-like	Salt
PL-10	33.34761	−115.96625	1.3	X	X	X		Playa-like/barnacle beach	Salt
PL-11	33.34793	−115.96646	1.3	X	X	X		Playa-like/ barnacle beach	Salt
PL-12	33.35158	−115.97068	2.7	X	X	X	X	Playa-like	Salt
BB-1	33.43991	−115.84320	1.0	X	X	X		Barnacle beach	Silt/clay
BB-2	33.08948	−115.70950	1.0	X	X	X		Barnacle beach	Salt
ID-1	33.18045	−115.85243	33.0	X	X	X		Dune–interdune	Silt/clay

activity (pH) of the soil was measured from a 1:1 soil–aqueous matrix suspension. Organic carbon was determined by loss on ignition (LOI), which determines a percent weight loss following combustion for 1 h at 600 °C (Ben-Dor and Banin, 1989). This loss was assumed to be soil organic matter, however it is noted that the results of this (and other) method(s) will over-estimate the percent organic matter when hydrated salt minerals are present.

Extractable cations (K, Mg, Ca, Na) and sulfate were measured using extraction and analysis. Phosphorus was measured using the sodium carbonate fusion method, which is a better method for soils with pH > 7.5 (in which case, extraction of P using the dilute acid fluoride method performs unsatisfactorily; Kuo, 1996). Cation exchange capacity (CEC) was determined using the ammonium saturation method (Sumner and Miller, 1996). The sodium adsorption ratio (SAR) was calculated as $[Na^+]/([Ca^{2+}] + [Mg^{2+}])^{1/2}$ (Sumner and Miller, 1996).

4. Results and discussion

The repeated field measurement campaigns yielded results that are compared across sites as well as at the same sites during the different field visits of SE05, JA06, MR06, and FE07. In the following discussion, each site is assigned a landform type to aid in classifying the quantitative results, while all soil measurements that were

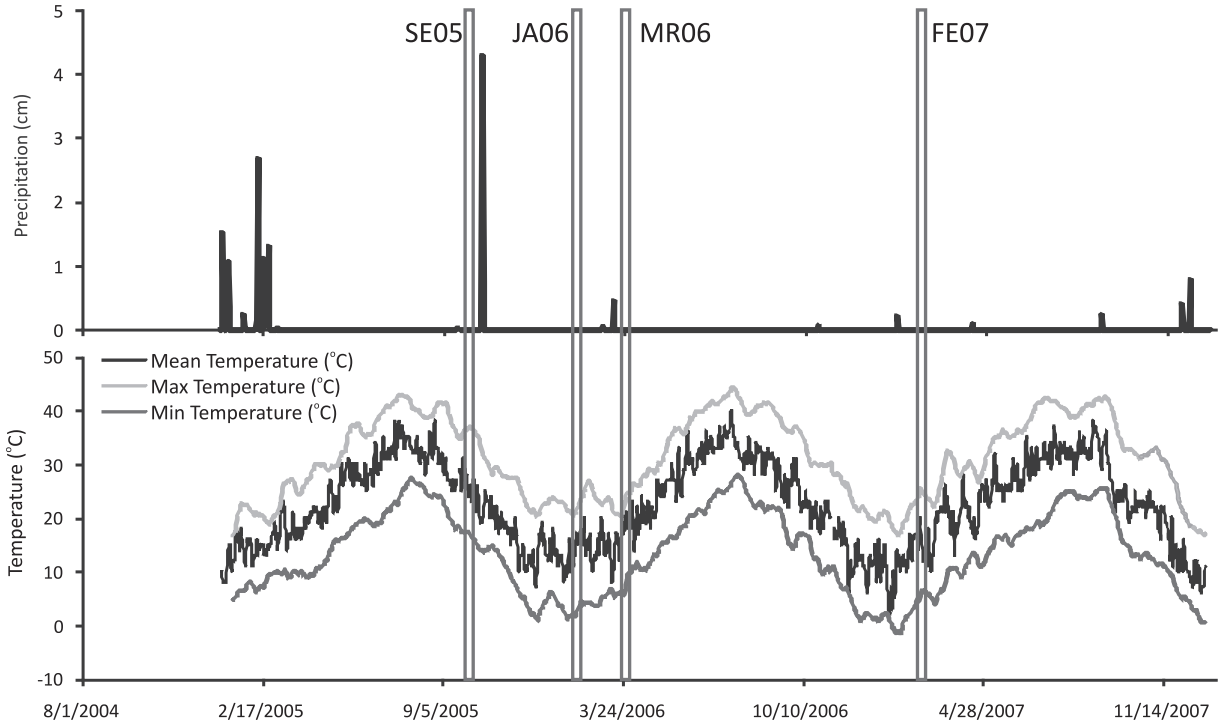

Fig. 3. Climatic data for the duration of the study period including mean daily temperature, 15-day moving average minimum and maximum temperature in degrees Celsius (°C), and daily total precipitation in centimeters (cm).

obtained by the laboratory analyses are summarized. Lastly, results from PI-SWERL potential wind erodibility tests with respect to PM_{10} dust emissions are given.

4.1. Site descriptions

Table 1 includes the landform classification, elevation, and crust type measurements that were completed at each site where wind erodibility measurements occurred. Testing occurred during four different field campaigns to represent seasonal variability in temperature and precipitation (Fig. 3).

4.2. Bulk analysis results

This section summarizes the results of bulk physical and chemical analysis of soil samples procured over the course of this study

Table 2
Site and field campaign specific surface soil properties including: soil moisture (%), organic matter (%), carbonate or $CaCO_3$ (%), pH, concentrations (ppm) of phosphorous (P) ions, potassium (K) ions, magnesium (Mg) ions, calcium (Ca) ions, sodium (Na) ions, and sulfate (SO_4) ions, soil texture (% sand, silt and clay), and salt content (mg/kg).

Site	Soil moisture (%)				Organic matter (%)				Carbonates (%)				pH			
Name	SE05	JA06	MA06	FE07	SE05	JA06	MA06	FE07	SE05	JA06	MA06	FE07	SE05	JA06	MA06	FE07
BB1	0.6	0.3	0.4		0.50	0.50			10.42	6.07	6.98		7.80	7.80		
BB2	4.0	5.2	4.3		2.30				27.09	27.98	35.98		8.00			
DW1	0.3	0.2	0.4		0.20	0.30	0.40		4.61	3.55	3.17		8.90	8.50	8.40	
DW2	0.3	0.9	1.8		0.40	0.40	0.30		4.39	7.38	6.71		8.10	8.30	8.50	
ID1	0.5	0.6	0.7		0.40	0.50	0.30		3.84	4.12	3.72		8.10	7.80	8.00	
PA1	1.4	1.8	3.1		1.00	1.20	0.90		17.78	10.06	16.22		8.40	7.70	7.70	
PA2	2.6	1.8	2.9	1.0	0.90	1.10	1.10	1.58	19.48	13.45	15.65	3.06	8.30	7.90	7.90	7.41
PL1	3.8	6.8	31.3	8.0	13.00	8.80	4.10	13.50	22.89	22.34	3.30	6.36	8.20	7.90	8.50	7.34
PL2				8.4				14.14				5.80				7.22
PL3				7.3				16.02				6.83				7.25
PL4	5.6	21.7	30.7	8.0	1.10	1.20	1.10	9.16	12.04	11.21	9.77	6.37	8.00	8.20	8.00	7.30
PL5	8.4	4.1	62.8	2.5	2.30	2.50	2.90	4.51	5.05	4.59	5.24	3.81	7.80	7.80	7.90	7.62
PL6	2.7		32.9	8.2	3.10		1.70	10.47	13.74		10.58	16.06	8.00		8.60	7.44
PL7		29.9	42.2	6.9		5.40	4.40	9.89		13.69	14.83	11.83		8.00	8.40	7.35
PL8		32.3	39.8	4.7		7.40	6.00	12.55		5.02	10.68	4.91		8.00	8.40	7.18
PL9		46.7	12.2	16.8		7.20	7.40	15.37		20.11	21.11	4.56		8.60	8.40	6.77
PL10	8.6	9.5	5.7		0.70	0.60	0.70		3.31	2.12	2.94		8.20	8.10	8.20	
PL11	2.8	0.8	6.3		1.20	0.40	0.80		2.90	4.76	2.80		8.50	8.20	8.50	
PL12	7.4	3.1	12.2	11.9	0.30	0.90	1.00	11.23	2.81	2.78	3.86	4.01	8.20	8.40	8.20	7.05

	P (ppm)				K (ppm)				Mg (ppm)				Ca (ppm)			
BB1	21	9			129	46			162	139			3991	4923		
BB2	16				97				189				30,250			
DW1	7	6	4		49	49	92		46	208	226		1010	1307	1496	
DW2	14	5	7		56	98	76		78	255	142		1197	2799	1936	
ID1	13	6	11		117	103	206		106	146	320		1993	1644	2883	
PA1	12	7	13		384	332	394		212	243	372		3967	3761	5285	
PA2	12	11	20		541	388	701		416	472	453		4718	3896	4281	
PL1																
PL2																
PL3																
PL4	12	8			575	694			758	1731			5131	4915		
PL5	10	13	15		1361	1536	1896		5640	4458	4551		3951	3526	3745	
PL6	24				353				2456				6286			
PL7		56				1254				4785				9631		
PL8		36				1100				4839				7042		
PL9																
PL10	13	11			398	216			758	905			3188	8400		
PL11	22	11	8		450	175	152		672	205	556		12,067	3168	8327	
PL12	10	6	8		249	360	147		734	2441	798		3377	2886	4892	

	Na (ppm)				SO_4 (ppm)				Soil texture (%)			Salt cont ent (mg/kg)			
	SE05	JA06	MA06	FE07	SE05	JA06	MA06	FE07	Sand	Silt	Clay	SE05	JA06	MA06	FE07
BB1	826	230			1605	3326			84.0	10.4	6.3	5423	5508	5431	
BB2	997				20,140				68.3	20.9	11.3	18,828	40,837	51,674	
DW1	80	1323	3084		9	650	1060		93.6	4.6	2.4	242	1001	970	
DW2	389	1186	654		177	1141	172		90.2	6.9	3.3	327	658	888	
ID1	48	385	1654		20	221	675		65.0	18.9	16.6	352	1218	443	
PA1	1964	1979	2392		588	676	1832		11.4	46.3	42.4	8071	886	18,554	
PA2	1950	1370	2366		310	550	650		6.7	52.8	40.5	1264	1074	6752	108,396
PL1									17.2	64.2	18.8	281,217	216,829	314,270	296,744
PL2									5.4	49.8	44.8				58,004
PL3									20.7	48.7	30.6				68,267
PL4	6220	10,180			3871	7083			7.9	43.2	48.8	28,682	81,441	178,401	378,464
PL5	10,970	10,650	10,430		21,125	31,120	30,280		1.4	36.6	62.0	206,509	300,807	333,532	585,969
PL6	8534				6783				18.1	58.2	23.7	90,434		65,044	353,884
PL7		10,730				29,680			13.6	55.1	31.2		306,273	220,062	522,389
PL8		10,910				30,000			19.5	63.1	17.3		326,725	211,472	603,111
PL9									18.6	60.7	20.8		176,799	179,257	512,717
PL10	8492	6871			6637	9412			81.4	13.5	5.3	76,491	190,354	94,287	
PL11	5854	808	4526		9807	1044	8514		72.8	19.9	7.5	75,291	4685	61,855	
PL12	9687	9319	7835		4386	10,700	5392		79.8	14.4	6.0	101,798	87,748	90,284	520,109

including soil moisture, particle size distribution, and soil chemical properties.

4.2.1. Soil moisture

The soil moisture content measured at each site only represented the bulk moisture in the top 30 cm of the soil. This measurement was made not to directly relate to dust emission processes, but to help categorize the landform and infer the effect of rainfall on each of the different sites. Surface soil moisture was not collected because of the complexities associated with accurately separating available moisture content from hydrated salt crusted surfaces. Sites higher in elevation than the Salton Sea water level have lower moisture content than the sites adjacent to the shoreline (Table 2). These lower moisture content sites are associated with paleolake, barnacle beach, dry wash, and interdune sites, while the sites with higher moisture levels are represented by the playa-like landform. A seasonal variation exists in the moisture content at the playa-like sites, with MA06 having the highest average value and SE05 having the lowest average value. It should also be highlighted that the sites containing a high amount of soluble salts will have an inaccurate measurement of moisture content because there are no current methods available to distinguish soil water from water contained in hydrated salt minerals. Current lab methods measure water content gravimetrically after evaporation, and even at relatively low temperatures of 105 °C, many of these hydrated salt minerals become unstable, dissolve, release their water, and reprecipitate as an anhydrous salt mineral, potentially over-estimating the water content in these samples. Therefore comparisons between landforms can only be made at a coarse scale.

4.2.2. Particle size distribution

The sites tested at the Salton Sea display a range of textures related to the landform which they were associated, while multiple samples from the same site are relatively homogeneous in textural quality. Loose surface soil aggregates were only observed at three sites (PL-7, PL-8, PL-12), on salty crusts, during JA06 testing. The aggregates appeared to be composed of sand or smaller particles cemented by salts. All other sites and sampling times had stable crusts with no discernible loose aggregates on the surface. With the exception of the sites PL-12, PL-11, and PL-10, playa-like sites were mostly composed of silt- and clay-sized sediments, while the other landforms of barnacle beach, dry wash, and interdune sites consisted of mainly sand-sized sediments (Table 2).

4.2.3. Soil chemical properties

Properties such as organic matter content (OM) and pH were relatively consistent within each site throughout the sampling period except for the playa-like sites. The sampled soils at all of the sites had low organic matter contents except for sites PL-1, JR1, PL-9, PL-7 and PL-8, which also contained abundant fish parts. Most sites showed consistent OM content throughout the testing, although they showed an increase in organic matter in the FE07 campaign. This increase in OM may be artificial due to the high amounts of hydrated salts. Currently, all methods to measure OM result in artificially high measurements in samples that contain hydrated salt minerals (see Buck et al., in press). Soils were on average moderately alkaline, with pH between about 6.8 and 8.9, at all sites during all seasons, with a non-statistically significant decreasing trend for most sites.

Soil chemistry was measured by extractable cations within the first three field campaigns, while the mineralogical content was measured using a different technique, not comparable to extraction for the February 2007 campaign and is only presented in Buck et al. (in review). Some of the extractable cation concentrations varied by several orders of magnitude from site to site. Variability among sites was significantly greater than variability from one season to the other at the same site. However, some differences in chemistry between different seasons at the same site were significant. Among P, Na, Ca, Mg, K, and SO_4, the most abundant ionic species were Na, Ca, and SO_4 with concentration ranges of 50–11,000 ppm, 1000–30,000 ppm, and 10–38,000 ppm, respectively. Concentrations of K, Mg, and P ions were generally lower with values in the ranges of 50–1900, 50–9000, and 4–160 ppm, respectively. With the exception of calcium, these species were present in approximately proportional quantities with some variation from one site to the next. Sites with the lowest concentrations were the dry wash and interdune sites, and sites with the highest concentrations were the playa-like and barnacle beaches.

Calcium carbonate percentages were relatively stable from season to season for most sites. Three sites showed large changes between sampling times (PL-1, PL-8, and PL-9), while PL-4 showed a steady decline in $CaCO_3$ content. Soils with high carbonate values (>10%) typically contained barnacles (BB-2, PL-1, PL-7) or snail shells (PA-1, PA-2). The sites with snail shells were deposits of ancient Lake Cahuilla ('paleolake' sites), and their higher carbonate contents could also be a function of their greater soil age (through pedogenic processes).

Salt content (mg/kg) measured by electrical conductivity (EC) did exhibit some spatial trends (Table 2). The highest salt contents were found at sites adjacent to the Salton Sea, where wicking and evaporation aided in their precipitation, or were contributed by sea spray or wave action. The Salton Sea has an average salinity of 45 g/L (Watts et al., 2001), which is more saline than seawater (~35 g/L) and the Colorado River (~1 g/L). Wind likely aided in drying newly precipitated salts, which were then available for transport as dust. It was observed that during windy days, salt-rich foam blew or washed shoreward, covering soils and providing another source of salt. Sites with high salt contents tended to form salt crusts when dry. Sites further from the shoreline tended to have low salt contents and crusts made of silt and clay. One exception to this rule was site BB-1, a barnacle beach site adjacent to the shoreline which contained barnacles, low salts, and silt/clay crusts. Influx of fresh water and sediment via ephemeral washes at this site may have kept salt levels in these soils low in addition to the shoreline being much steeper than the other sites. Temporally, no significant trends are observed in EC content at all sites, however, highest EC values in most cases tended to occur during January and February.

4.3. Potential PM_{10} emissions

This section summarizes the results from wind erodibility measurements performed with the PI-SWERL. Results are presented from several different perspectives. First, we summarize the potential PM_{10} emissions at different values of friction velocity. Second, we compare potential PM_{10} emissions measured at all the sites at a specific value of u^* to provide a context for the measurements in terms of their relative magnitudes, both at individual sites and when grouped by landform. For these results, arithmetic averages are calculated both on a per site basis and when data are aggregated by landform. Arithmetic averaging is more intuitive and is useful for quickly determining how important a specific value of PM_{10} emissions is in the context of all the data.

Using the maximum roughness height for all sites ($z_0 = 6.2 \times 10^{-4}$ m) in conjunction with the maximum measured one-hour wind speed at the Salton Sea and measurements with a field wind tunnel (Etyemezian et al., 2006) provides a maximum reasonable value of average one-hour friction velocity for exposed soil surfaces at the Salton Sea of $u^* = 0.56$ m/s. This value of friction velocity was chosen for comparing emissions from all sites at the Salton Sea by landform. It is noted however, that short-term

Table 3
Geometric mean and geometric standard deviation potential PM_{10} emissions ($mg/m^2/s$) measured at a shear velocity of 0.56 m/s given for each site and field campaign.

Site	September 2006		January 2007		March 2007		February 2008	
	Mean	σ	Mean	σ	Mean	σ	Mean	σ
PA-1	0.019	2.196	0.034	1.548	0.031	14.070		
PA-2	0.004	1.157	0.010	5.948	0.005	1.549	0.010	1.415
PL-1							0.262	1.993
PL-2							0.019	2.130
PL-4	0.006	1.478	0.150	1.903			0.087	1.736
PL-5	0.013	3.443	0.026	3.184	0.003	1.437	0.030	1.301
PL-6	0.004	2.650						
PL-7			1.426	3.290			0.179	3.048
PL-8			0.107	1.908			0.901	1.666
PL-9			0.239	5.546			0.011	1.749
PL-10	0.005	3.481	0.359	1.942	0.006	1.116	0.008	1.301
PL-11	0.034	4.143	2.459	1.137	0.017	5.200		
PL-12	0.008	2.763	0.060	1.476	0.202	3.013	0.011	1.696
BB-1	0.073	9.136	0.139	2.203	0.006			
BB-2	0.006	1.675	0.185	2.721	0.023	1.998		
DW-1	0.328	2.850	0.826	1.424	0.097	1.168		
DW-2	0.389	3.590	1.466	2.155	0.382	2.554		
ID-1	0.016	2.106	0.269	1.252	0.279	1.511		

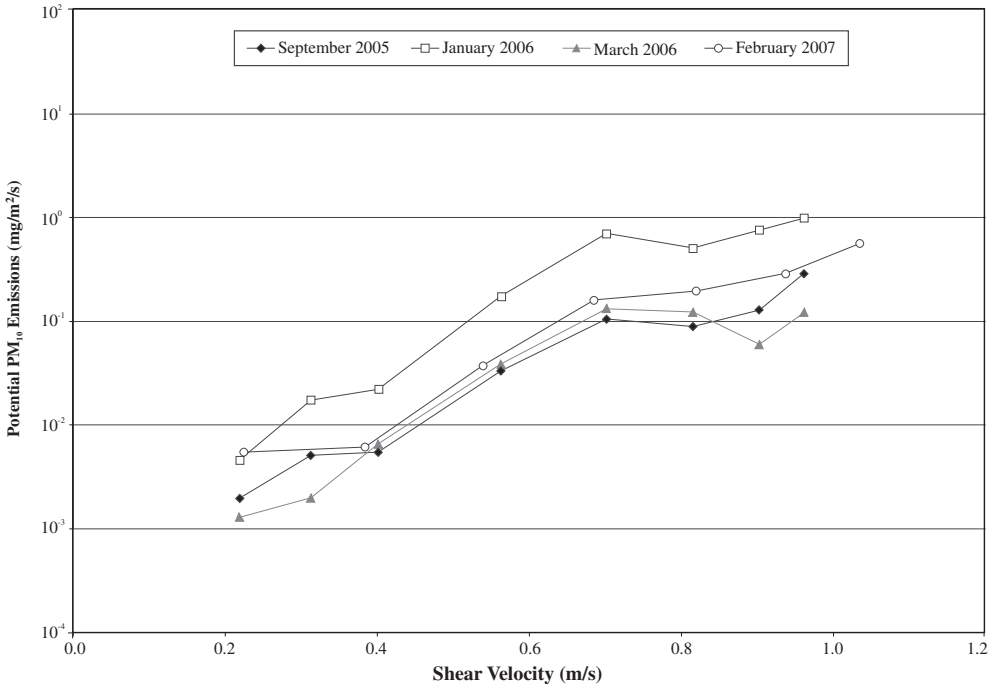

Fig. 4. Potential PM_{10} dust emissions for each sampling season as measured by the PI-SWERL.

sustained winds (e.g., 10 min) could result in substantially higher friction velocities (>0.7 m/s) and that occasional wind gusts (5–30 s) may intermittently cause much higher equivalent friction velocities (>0.9 m/s). Therefore, $u^* = 0.56$ m/s does not represent a strict upper limit on the reasonable range of friction velocities that can occur at the Salton Sea. Additionally, the assumed roughness for all sites is used for determining the equivalent shear velocity within the PI-SWERL and variations in the actual roughness during the tests may cause some variation in the actual friction velocity occurring in the PI-SWERL (however, $a \pm 10\%$ variation around the assumed roughness translates to only $a \pm 2\%$ change in 10 m high equivalent wind velocity).

PI-SWERL potential PM_{10} emissions, averaged for all sites, are segregated by field sampling season in Table 3. The data correspond to the geometric mean of potential PM_{10} emissions from all replicate tests at the specified friction velocity. Overall, the potential PM_{10} emissions were generally lowest in September 2005 and March 2006, while slightly higher values were measured in February 2007 and the highest measured in January 2006. Although no season was significantly more emissive than another season when all landforms are included in the average ($\alpha = 0.05$). These values of potential PM_{10} emissions for the range of shear velocity tested are displayed in Fig. 4 on a logarithmic scale.

Table 3 shows individual sites averaged geometrically for replicate tests and the geometric standard deviation of PM_{10} emissions for each site for all the seasons measured. Although not all sites were visited during each field visit, the replicate measurements seem to have provided a good indication of the inter- and intra-site variability. Over all seasons when measurements were made, the DW and ID landforms have a significantly greater ($\alpha = 0.05$) rate of emissions with shear velocity than both the PL and PA landforms, while the BB landform also exhibits a greater rate of

increase than the PL landform. If each season and landform are analyzed separately (for the seasons where all landforms were tested: SE05, JA06, MR06), the DW landform had a greater rate of emissions than PL and PA landforms for the SE05 and MR06 seasons, while during JA06 no landform was significantly different ($\alpha = 0.05$).

5. Discussion

5.1. Data trends: season and salt content

In Fig. 5, sites have been plotted by salt content and PM_{10} emissions for each of the four field campaigns. For the purposes of comparison, sites that were considered as having low salt content (salt by EC < 10,000 mg/kg) for any visit during the field campaign included DW-2, PA-1, PA-2, BB-1, PA-1, DW-1, and ID-1. Among those locations, sites BB-1, DW-2, DW-1, and ID-1 contained low salt content throughout all field campaigns. Sites with relatively high salt content (salt by EC > 10,000 mg/kg) included PL-4 through PL-12, and BB-2.

A number of interesting patterns can be seen Fig. 5. First, the potential PM_{10} emissions are higher for both salt-rich and low-salt soils in January compared to the other field visits. Second, the magnitude of PM_{10} emissions in January is not significantly different between salt-rich and low-salt sites. Third, mean PM_{10} emissions for salt-rich sites are lower than those at low-salt sites in September and March (although not significant). Therefore the magnitudes of the salt content, as measured by EC, are not able to predict the absolute values of PM_{10} emissions for the range of sites and periods tested even for very salty soils.

5.2. Magnitudes of PM_{10} emissions by site and by landform

Examination of PM_{10} emissions at various sites on an absolute scale (linear scale) can provide insight into the relative importance of specific landforms in terms of overall emissions in an air shed. However, by calculating the geometric standard deviation for the replicate measurements, the range of values around the geometric mean can also be realized. Table 3 shows all PM_{10} emission measurements at all the sites for each of the four sampling seasons at a friction velocity (u^*) of 0.56 m/s and includes the geometric standard deviations of replicate measurements. The data show that the range of PM_{10} emissions at some sites are orders of magnitude higher than other sites – this is indicated by the geometric standard deviation, which expresses an order of magnitude variation with every integer increase. In addition, the rather large variability in PM_{10} emissions over multiple measurements within the same site is conveyed by the magnitude of the standard deviation as compared to the value of the averages.

The geometric standard deviation (GSD) does not show any discernible trends in terms of the different landforms. In addition, all landforms except the paleo-lake (PA) landform showed no

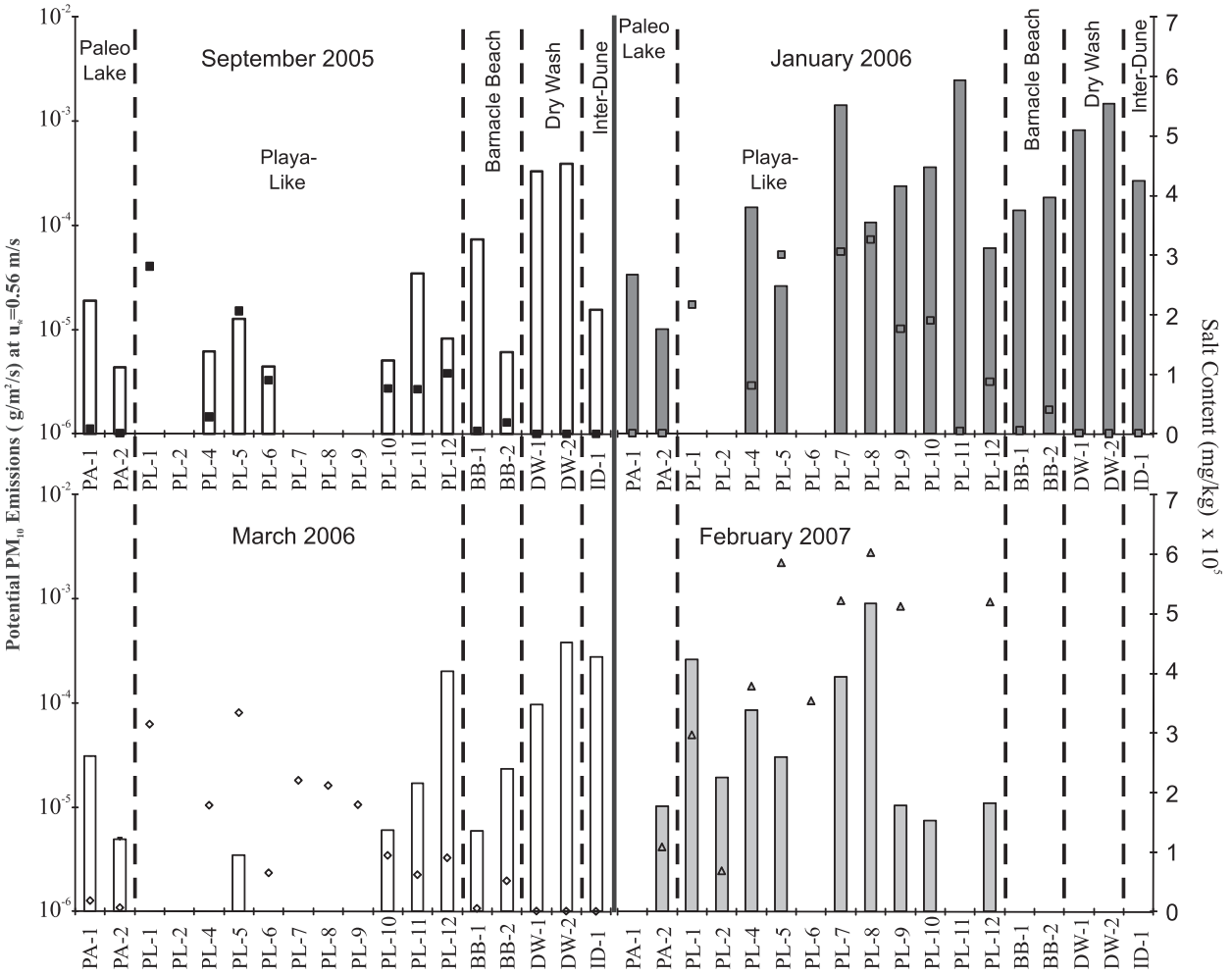

Fig. 5. Potential PM_{10} dust emissions at a shear velocity of 0.56 m/s (primary *y*-axis) separated for each field campaign and separated for each site location (*x*-axis) as vertical bars, with salt content (mg/kg) plotted on the secondary *y*-axis as symbols.

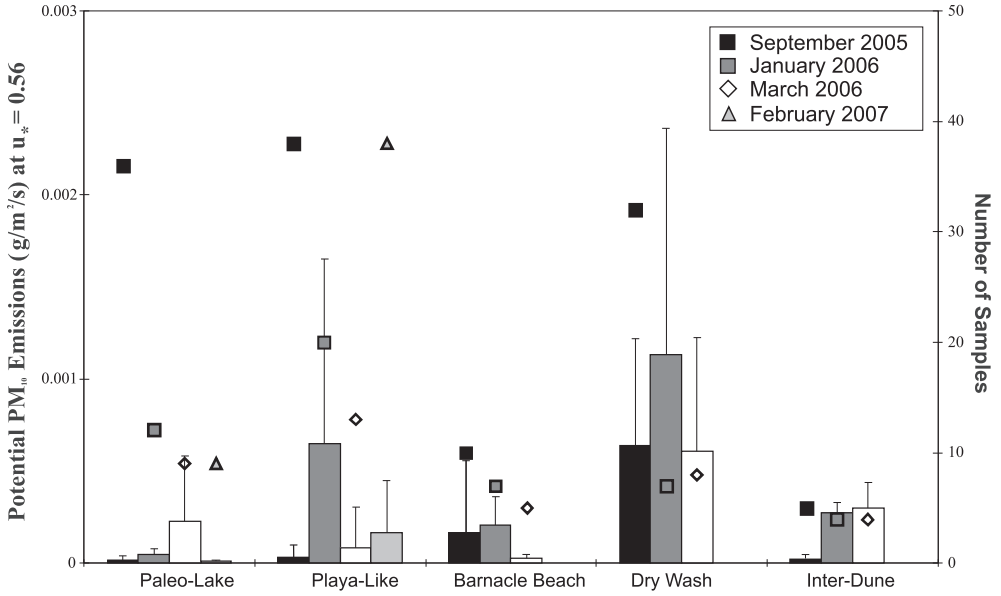

Fig. 6. Averaged PM_{10} dust emissions at a shear velocity of 0.56 m/s for each landform classification separated by field campaign season and include standard error bars. Also plotted (open symbols), but on the secondary *y*-axis, are the number of samples taken associated with the average and standard error values.

significant difference in potential PM_{10} emissions at a u^* of 0.56 m/s over the different measurement campaigns. At a number of sites where measurements were completed in September 2005, the GSD appears to be elevated compared to other sites and compared to the same sites in January and March. The reason for this is unknown, though we note that for sites BB-1, PL-5, PL-10, and PL-11 – three of the sites with the highest GSD values in September – the average emissions at $u^* = 0.56$ m/s were quite low compared to other sites. This suggests that these large values of CV for some of the September measurements would not have an impact on windblown dust emission estimates for the Salton Sea basin. Furthermore, the lower values attributed to a portion of the larger GSD might be approaching the measurement accuracy limit of the PI-SWERL resulting in the larger apparent variability at a site.

Average values of potential PM_{10} emissions are shown by landform grouping rather than by individual site in Fig. 6. Despite the large standard deviations associated with those data, the relatively large number of data points adds strength to the conclusion that the increases in potential PM_{10} emissions during the January tests were a result of the playa-like and, to a lesser extent, the dry wash landforms. Fig. 6 shows that on average, the highest PM_{10} emissions at $u^* = 0.56$ m/s are at dry wash landforms (significant at $\alpha = 0.05$) for all measurement periods. Playa-like sites also exhibit significantly higher emissions in JA06 compared to the SE05 and MR06 months ($\alpha = 0.05$), though we note that some sites are not represented in all the averages for the three seasons. For example, site PL-8 is a significant contributor to the high average emissions in January, but PL-8 was not tested in September (underwater) and was too wet to test in March but was the largest emitter in February 2007. Thus it is difficult to determine from the data if all playa-like sites were more emissive in January than in March or September or if the high average emissions in January were strictly driven by sites like PL-8 that could not be consistently sampled. This further complicates projecting the measured potential emissions as representative values for the landforms combined with the natural wind regime for a regional contribution PM_{10} emission map.

5.3. Salton Sea dust emission potential

The relative amounts of potential dust production from this study have shown that some degree of seasonality can be attributed to type of landforms that a surface is associated with, however the magnitude of these emissions have not been qualified through comparison with other studies. Fig. 7 shows a scatter plot grouped by experiment of potential and fugitive PM_{10} dust emissions ($g/m^2/s$) as a function of u^* (m/s). The data collected from other studies include field data (Niemeyer et al., 1999) and portable wind tunnel data (Nickling and Brown, 2001) on Owens Lake, portable wind tunnel data from both the University of Guelph wind tunnel and the PI-SWERL from various surfaces within the Mojave National Preserve and the Salton Sea from April to September 2005 (Sweeney et al., 2008), and a laboratory wind tunnel with Owens Lake soils (Roney and White, 2006). This collection of reported PM_{10} emissions demonstrates the large variation of emission rate with shear velocity with the best-fit power curves ($F = a(u^*)^b$) of the data groups, with coefficients ranging from $b = 1.43$ (Sweeney et al., 2008 Guelph wind tunnel) to $b = 5.76$ (Niemeyer et al., 1999). Theoretical and experimental models that use saltation bombardment to explain the dust emission process express the ratio of saltating sand particles in a horizontal flux (q) ($q = f(u^{*3})$) to the vertical dust flux as independent of shear velocity for a given soil condition and type. This contrasts the experimental data in Fig. 7, except only that of Gillette and Passi (1988) with an exponent of $b = 3$ (making the dust emissions independent of u^* in the saltation bombardment approach), suggesting other processes occurring in addition to those that the saltation bombardment process can explain. This discrepancy has also been found in disturbed clay-crusted soils by Houser and Nickling (2001) although with PM_{10} emission rates below that of the sediment transport rate. This suggests that dust emissions from salt-crusted or salt-rich depressions within the U.S. southwest tend to have a larger vertical dust flux for the same u^* than non-saline soils. Although visually some distinctions exists between the data groups, only the January 2007 portion of the Salton Sea data from this study (not shown separately) is significantly greater than the Sweeney et al. (2008) Guelph wind tunnel and PI-SWERL data. Equally important is the PM_{10} emission data of Niemeyer et al. (1999) that are substantially greater for the same u^*. In contrast, other sources report dust emissions related to shear velocity for both wind tunnels and measured fugitive emissions that are close to a value of $b = 3$ (Gillette, 1978; Nickling, 1978; Nickling and Gillies, 1989; Houser and Nickling, 2001; Ono, 2006). The exponents for the dust emissions from

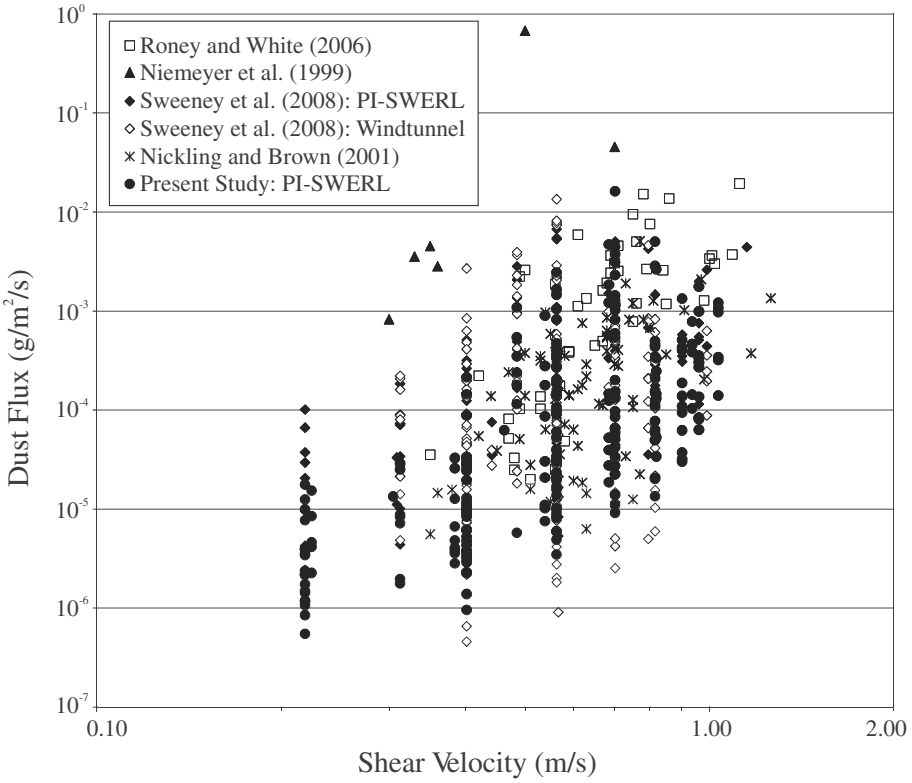

Fig. 7. Dust flux ($g/m^2/s$) plotted against shear velocity (m/s) for the present study as one group and other published data.

experiments measuring the total suspended particulate (TSP) concentration tended to have values closer to a value of 3, while those measuring PM_{10} tend to have values greater than 3. Houser and Nickling (2001) suggest that it is not the shear velocity that ultimately controls the dust emission but the availability of loose erodible particles to impact and aid in releasing the dust. The seasonality of the PM_{10} emissions from crusted surfaces measured in this report agrees with the dependence of the emissions on surface conditions rather than shear velocity. However, for the surfaces that do not exhibit any physical crusts the shear velocity explains the PM_{10} dust emissions (using the approach from above: $F = a(u^*)^b$) relatively well ($R^2 = 0.78$ for all tests from the DW sites) for this study compared to the all of the sites ($R^2 = 0.47$). It is the smaller footprint and higher level of control available to the PI-SWERL instrument responsible for producing this strong relationship. This level of control is not available to much larger wind tunnels and field studies because of averaging emissions over much larger spatial and temporal periods, which is evident in the scatter of the previously available data.

6. Conclusions

At the Salton Sea, soft crusts were found to be significant producers of dust during winter and early spring, as were dry wash areas containing loose particles on the surface year-round. The removal of fluffed salts by wind erosion facilitates the bare soil to continue salt formation, similar to the processes at Owens Lake, appears to be operating along exposed shores of the Salton Sea.

Our research plan allowed measurement of dust and soil properties four different times of year over 3 years, to reflect potential seasonal changes in dust emissions. The data show that dust emissions were higher in the winter months (especially January 2006) compared to summer and spring at the Salton Sea. Ten of the 16 sites where PI-SWERL measurements were completed exhibited their highest dust fluxes in January (PA-1, PL-4, PL-7, PL-9, PL-10, PL-11, DW-1, DW-2, BB-1, BB-2). Of those, five had silt/clay crusts (low salt) and five had salt-based crusts. One site had their highest measured dust emissions in September (PL-6; silt/clay), two sites had their highest measured dust emissions in March (PL-12; salt crust, ID-1; silt/clay), and three in February (PL-5, PL-8; salt crust, PA-2; silt/clay). Of the 11 sites with the overall highest emissions (PL-4, PL-7, PL-8, PL-9, PL-10, PL-11, DW-1, DW-2, PA-1, ID-1, BB-1), two had no crust, two had silt/clay crusts and six had salt crusts. For the most part, sites with silt/clay crusts or no crust showed the most consistent emissions from season to season with minor variation. Salt-dominated crusts showed the most variation, with the largest PM_{10} emissions occurring in the winter.

No clear correlation was evident between PM_{10} emission and soil texture. The highest emissions came from soils with textures ranging from sand to silty clay. Similarly, some of the lowest emissions came from sites with a similar spread in texture. This is additional supporting evidence that crusts are a major influence on fugitive dust production, perhaps more important than soil texture in many cases.

Sites were also grouped by five landform types. Those were playa-like, paleolake, barnacle beach, dry wash, and interdune. Playa-like sites were considered to most closely resemble what the sediment in the Salton Sea would be like immediately after water levels recede. When comparing PM_{10} emissions among these landform types at a common friction velocity of 0.56 m/s – a reasonable upper end value for the conditions of the Salton Sea – dry wash sites consistently exhibited the highest PM_{10} emissions during the three field campaigns in which they were sampled. However, average emissions from playa-like sites in January 2006 were comparable to those from dry wash sites owing to the formation of a friable crust at many of the playa-like sites in the cool, wet conditions of the season.

Our study suggested that while salt-crusted surfaces do indeed emit dust, they were not the single predominant source of dust around the margin of the Salton Sea. Most types of crusts appeared to become weaker during the winter as a function of temperature and humidity, but not as a function of salt mineralogy or absolute salt content. There appear to be other factors that influence how salt crusts behave (Buck et al., in press).

The Salton Sea salt-based crusts near the shoreline appeared to be significant but temporary sources of dust, limited to cool, wet months, whereas silt/clay crusted sites and dry washes (not only limited to playa-like environments) appeared to be significant sources of dust throughout the year.

Acknowledgements

The authors thank Bill Nickling and Jack Gillies for their assistance during the field study and input throughout the study. The authors gratefully acknowledge the helpful comments, critiques and suggestions provided by John Dickey, Carrie MacDougall, Mark Schaaf, and Pamela Vanderbilt (CH2 M Hill), Pat Chavez (USGS), Cheryl Rodriguez (BOR), Ted Schade (GBUAPCD), and Nick Lancaster (DRI). We deeply appreciate the time that Mr. Al Kalin spent conveying valuable insights into locations of playas and seasonality of dust emissions. The assistance of Mr. Bruce Wilcox (IID) in obtaining permission to perform measurements on IID-managed property was critical to the timely completion of this study. We would like to express our gratitude for the administrative and logistical support that was necessary to complete this project and was provided by Charles Keene, Jerry Boles, John Vrymoed, and Jeanine Jones (DWR). This work was funded through contract with the California Department of Water Resources (Standard Agreement No. 4600003670, Task Order No. SS0405-3670-0003).

References

Babcock, E.A., 1974. Geology of the northeast margin of the Salton trough, Salton Sea, California. Geological Society of America Bulletin 85, 321–322.

Bagnold, R.A., 1941. The Physics of Blown Sand and Desert Dunes. Methuen, London, 265p..

Ben-Dor, E., Banin, A., 1989. Determination of organic matter content in arid-zone soils using a simple "loss-on ignition" method. Communications in Soil Science and Plant Analysis 20, 1675–1695.

Buck, B.J., Wolff, K., Merkler, D.J., McMillan, N.J., 2006. Salt mineralogy of Las Vegas Wash, Nevada: morphology and subsurface evaporation. Soil Science Society of America Journal 70, 1639–1651.

Buck, B.J., King, J., Etyemezian, V., in press, Effects of salt mineralogy on dust emissions: Salton Sea California, USA, Soil Science Society of America Journal.

Dreimanis, A., 1962. Quantitative gasometric determinations of calcite and dolomite by using Chittick apparatus. Journal Sedimentary Petrology 32, 520–529.

Etyemezian, V., Sweeney, M., MacDonald, E., Nickling, W.G., Caldwell, T., Gillies, J., Macpherson, T., Nikolich, G., Xu, J., 2006. Measurement of windblown dust emission potential and soil characteristics at the Salton Sea in support of the Programmatic Environmental Impact Report, Final Report prepared for California Department of Water Resources.

Etyemezian, V., Nikolich, G., Ahonen, S., Pitchford, M., Sweeney, M., Purcell, R., Gillies, J., Kuhns, H., 2007. The Portable In-Situ Wind ERosion Laboratory (PI-SWERL): a new method to measure PM10 windblown dust properties and potential for emissions. Atmospheric Environment 41 (18), 3789–3796.

Gee, G.W., Or, D., 2002. Particle-size analysis. In: Dane, J.H., Topp, G.C. (Eds.), Methods of Soil Analysis: Part 4–Physical Methods, No. 5 Soil Sci. Soc. Am. Book Series. Soil Science Society of America, Madison, WI, pp. 255–293.

Gill, T.E., 1996. Eolian sediment generated by anthropogenic disturbance of playas: human impacts on the geomorphic system and geomorphic impacts on the human system. Geomorphology 17, 207–228.

Gillette, D.A., 1978. A wind tunnel simulation of the erosion of soil: effect of soil texture, sand-blasting, wind speed, and soil consolidation on the dust production. Atmospheric Environment 12, 1735–1743.

Gillette, D.A., 1979. Environmental factors affecting dust emission by wind erosion. In: Morales, C. (Ed.), Saharan Dust. Wiley, Chichester, pp. 71–91.

Gillette, D.A., Chen, W., 1999. Size distributions of saltating grains: an important variable in the production of suspended particles. Earth Surface Processes and Landforms 24, 449–462.

Gillette, D.A., Passi, R., 1988. Modeling dust emission caused by wind erosion. Journal of Geophysical Research 93 (D11), 14233–14242.

Gillette, D.A., Walker, T., 1977. Characteristics of airborne particles produced by wind erosion of sandy soil, high plains of West Texas. Soil Science 123, 97–110.

Gillette, D.A., Adams, J., Muhs, D., Kihl, R., 1982. Threshold friction velocities and rupture moduli for crusted desert soils for the input of soil particles in the air. Journal of Geophysical Research 87 (C11), 9003–9015.

Gillette, D.A., Ono, D., Richmond, K., 2004. A combined modeling and measurement technique for estimating windblown dust emissions at Owens (dry) Lake, California. Journal of Geophysical Research 109(F01003). doi:10.1029/2003JF000025.

Gomes, L., Bergametti, G., Coude-Gassen, G., Rognon, P., 1990. Submicron desert dust: a sandblasting process. Journal of Geophysical Research 95 (D9), 13927–13935.

Houser, C.A., Nickling, W.G., 2001. The factors influencing the abrasion efficiency of saltating grains on a clay-crusted playa. Earth Surface Processes and Landforms 26, 491–505.

Kunze, G.W., Dixon, J.B., 1986. Pretreatment for mineralogical analysis. In: Arnold, K. (Ed.), Methods of Soil Analysis: Part I. Physical and Mineralogical Methods, Agronomy, vol. 9. American Society of Agronomy, Inc. and Soil Science Society of America, Inc., Madison, WI, pp. 91–100.

Kuo, S., 1996. Phosphorous. Methods of Soil Analysis Part 3: Chemical Methods, SSSA Book Series No. 5, pp. 869–920.

Langston, G., McKenna Neuman, C., 2005. An experimental study on the susceptibility of crusted surfaces to wind erosion: a comparison of the strength properties of biotic and salt crusts. Geomorphology 72, 40–53.

Loosemore, G.A., Hunt, J.R., 2000. Dust resuspension without saltation. Journal of Geophysical Research 105(D16), 20663–20671.

Lu, H., Shao, Y., 1999. A new model for dust emission by saltation bombardment. Journal of Geophysical Research 104(D14), 16827–16842.

Machette, M.N., 1986. Calcic soils of the southwestern United States. Geological Society of America Special Paper 203, 1–21.

Nickling, W.G., 1978. Eolian sediment transport during dust storms: Slims River Valley, Yukon Territory. Canadian Journal of Earth Science 15, 1069–1084.

Nickling, W.G., 1984. The stabilizing role of bonding agents on the entrainment of sediment by wind. Sedimentology 31, 111–117.

Nickling, W.G., Brown, L.S., 2001. PM_{10} dust emissions at Owens Lake CA, Final Report. 75p.

Nickling, W.G., Gillies, J.A., 1989. Emission of fine grained particles from desert soils. In: Leinen, M., Sarnthein, M. (Eds.), Palaeoclimatology and Palaeometerology: Modern and Past Patterns of Global Atmospheric Transport. Amsterdam, Kluwer, pp. 133–165.

Nickling, W.G., Lancaster, N., Gillies, J.A., 1997. Field Wind Tunnel Studies of Relations Between Vegetation Cover and Dust Emissions at Owens Lake, Report to the Great Basin Unified Air Pollution Control District. Bishop, California.

Niemeyer, T.C., Gillette, D.A., DeLuisi, J.J., Kim, Y.J., Niemeyer, W.F., Ley, T., Gill, T.E., Ono, D., 1999. Optical depth, size distribution and flux of dust from Owens Lake, California. Earth Surface Processes and Landforms 24, 5.

Okin, G.S., 2005. Dependence of wind erosion and dust emission on surface heterogeneity: Stochastic modeling. Journal of Geophysical Research 110, D11208, doi:10.1029/2004JD005288.

Ono, D., 2006. Application of the Gillette model for windblown dust at Owens Lake, CA. Atmospheric Environment 40, 3011–3021.

Pelletier, J.D., 2006. Sensitivity of playa windblown-dust emissions to climatic and anthropogenic change. Journal of Arid Environments 66 (1), 62–75.

Reynolds, R., Yount, J.C., Reheis, M., Goldstein, H., Chavez, P., Fulton, R., Whitney, J., Fuller, C., Forester, R.M., 2007. Dust emission from wet and dry playas in the Mojave Desert, USA. Earth Surface Processes and Landforms 32 (12), 1811–1827.

Rice, M.A., McEwan, I.K., 2001. Crust strength: a wind tunnel study of the effect of impact by saltating particles on cohesive soil surfaces. Earth Surface Processes and Landforms 26, 721–733.

Rice, M.A., McEwan, I.K., Mullins, C.E., 1999. A conceptual model of wind erosion of soil surfaces by saltating particles. Earth Surface Processes and Landforms 24, 383–392.

Richards, L.A. (Ed.), 1954. Diagnosis and improvement of saline and alkali soils. Agricultural Handbook No. 60. U.S Department of Agriculture. U.S. Government Printing Office, Washington, D.C.

Roney, J.A., White, B.R., 2006. Estimating fugitive dust emission rates using an environmental boundary layer wind tunnel. Atmospheric Environment 40 (40), 7668–7685.

Schoeder, R.A., Orem, W.H., Kharaka, Y.K., 2002. Chemical evolution of the Salton Sea, California: nutrient and selenium dynamics. Hydrobiologia 473, 23–45.

Shao, Y., Lu, H., 2000. A simple expression for wind erosion threshold friction velocity. Journal of Geophysical Research – Atmospheres 105(17), 22437–22443.

Shao, Y., Raupach, M.R., Findlater, P.A., 1993. Effect of saltation bombardment on the entrainment of dust by wind. Journal of Geophysical Research 98 (D7), 719–721.

Soil Survey Division Staff, 1993. Soil Survey Manual. United States Department of Agriculture, 457p.

Soukup, D.A., Buck, B.J., Harris, W., 2008. Preparing soils for mineralogical analyses. In: Ulery, A.L., Drees, L.R. (Eds.), Methods of Soil Analysis, Part 5 – Mineralogical Methods. Soil Sci. Soc. Am, Madison, WI, pp. 13–31.

Sumner, M.E., Miller, W.P., 1996. Cation exchange capacity and exchange coefficients. Methods of Soil Analysis Part 3: Chemical Methods, SSA Book Series No. 5, pp. 1201–1230.

Sweeney, M., Etyemezian, V., Macpherson, T., Nickling, W.G., Gillies, J.A., Nikolich, G., McDonald, E., 2008. Comparison of PI-SWERL with dust emission measurements from a single-line field wind tunnel. Journal of Geophysical Research. doi:10.1029/2007JF000830.

Watts, J., Swan, B.K., Tiffany, M.A., Hurlburt, S.H., 2001. Thermal, mixing, and oxygen regimes of the Salton Sea, California, 1997–1999. Hydrobiologia 466, 159–176.